Nanoscale Research Letters
a SpringerOpen Journal

NANO EXPRESS Open Access

Structural and electronic properties of germanene/MoS_2 monolayer and silicene/MoS_2 monolayer superlattices

Xiaodan Li[1,2], Shunqing Wu[1,2], Sen Zhou[3] and Zizhong Zhu[1,2*]

Abstract

Superlattice provides a new approach to enrich the class of materials with novel properties. Here, we report the structural and electronic properties of superlattices made with alternate stacking of two-dimensional hexagonal germanene (or silicene) and a MoS_2 monolayer using the first principles approach. The results are compared with those of graphene/MoS_2 superlattice. The distortions of the geometry of germanene, silicene, and MoS_2 layers due to the formation of the superlattices are all relatively small, resulting from the relatively weak interactions between the stacking layers. Our results show that both the germanene/MoS_2 and silicene/MoS_2 superlattices are manifestly metallic, with the linear bands around the Dirac points of the pristine germanene and silicene seem to be preserved. However, small band gaps are opened up at the Dirac points for both the superlattices due to the symmetry breaking in the germanene and silicene layers caused by the introduction of the MoS_2 sheets. Moreover, charge transfer happened mainly within the germanene (or silicene) and the MoS_2 layers (intra-layer transfer), as well as some part of the intermediate regions between the germanene (or silicene) and the MoS_2 layers (inter-layer transfer), suggesting more than just the van der Waals interactions between the stacking sheets in the superlattices.

Keywords: Superlattice; MoS_2 monolayer; Germanene; Silicene

Background

In the past decade, the hybrid systems consisting of graphene and various two-dimensional (2D) materials have been studied extensively both experimentally and theoretically [1-6]. It has long been known that the thermal, optical, and electrical transport properties of graphene-based hybrids usually exhibit significant deviations from their bulk counterparts, resulting from the combination of controlled variations in the composition and thickness of the layers [6,7]. Moreover, the use of 2D materials could be advantageous for a wide range of applications in nanotechnology [8-13] and memory technology [14-16]. Among those hybrid systems, the superlattices are considered as one of the most promising nanoscale engineered material systems for their possible applications in fields such as high figure of merit thermoelectrics, microelectronics, and optoelectronics [17-19]. While the research interest in graphene-based superlattices is growing rapidly, people have started to question whether the graphene could be replaced by its close relatives, such as 2D hexagonal crystals of Si and Ge, so called silicene and germanene, respectively. Silicene and germanene are also zero-gap semiconductors with massless fermion charge carriers since their π and π^* bands are also linear at the Fermi level [20]. Systems involving silicene and germanene may also be very important for their possible use in future nanoelectronic devices, since the integration of germanene and silicene into current Si-based nanoelectronics would be more likely favored over graphene, which is vulnerable to perturbations from its supporting substrate, owing to its one-atom thickness.

Germanene (or silicene), the counterpart of graphene, is predicted to have a geometry with low-buckled honeycomb structure for its most stable structures unlike the planar one of graphene [20-22]. The similarity among germanene, silicene, and graphene arises from the fact that Ge, Si, and C belong to the same group in the

* Correspondence: zzhu@xmu.edu.cn
[1]Department of Physics, Xiamen University, Xiamen 361005, China
[2]Institute of Theoretical Physics and Astrophysics, Xiamen University, Xiamen 361005, China
Full list of author information is available at the end of the article

periodic table of elements, that is, they have similar electronic configurations. However, Ge and Si have larger ionic radius, which promotes sp^3 hybridization, while sp^2 hybridization is energetically more favorable for C atoms. As a result, in 2D atomic layers of Si and Ge atoms, the bonding is formed by mixed sp^2 and sp^3 hybridization. Therefore, the stable germanene and silicene are slightly buckled, with one of the two sublattices of the honeycomb lattice being displaced vertically with respect to the other. In fact, interesting studies have already been performed in the superlattices with the involvement of germanium or/and silicon layers recently. For example, the thermal conductivities of Si/SiGe and Si/Ge superlattice systems are studied [23-25], showing that either in the *cross-* or *in-plane* directions, the systems exhibit reduced thermal conductivities compared to the bulk phases of the layer constituents, which improved the performance of thermoelectric device. It is also found that in the ZnSe/Si and ZnSe/Ge superlattices [26], the fundamental energy gaps increase with the decreasing superlattice period and that the silicon or/and germanium layer plays an important role in determining the fundamental energy gap of the superlattices due to the spatial quantum confinement effect. Hence, the studies of these hybrid materials should be important for designing promising nanotechnology devices.

In the present work, the structural and electronic properties of superlattices made with alternate stacking of germanene and silicene layers with MoS_2 monolayer (labeled as Ger/MoS_2 and Sil/MoS_2, respectively) are systematically investigated by using a density functional theory calculation with the van der Waals (vdW) correction. In addition, we compare the results of Ger/MoS_2 and Sil/MoS_2 superlattices with the graphene/MoS_2 superlattice [6] to understand the properties concerning the chemical trend with the group IV atoms C, Si, and Ge in the superlattices. Our results show that Ger/MoS_2 and Sil/MoS_2 consist of conducting germanene and silicene layers and almost-insulating MoS_2 layers. Moreover, small band gaps open up at the *K* point of the Brillouin zone (BZ), due to the symmetry breaking of the germanene and silicene layers which is caused by the introduction of the MoS_2 layers. Localized charge distributions emerged between Ge-Ge or Si-Si atoms and their nearest neighboring S atoms, which is different from the graphene/MoS_2 superlattice, where a small amount of charge transfers from the graphene layer to the MoS_2 sheet [6]. The contour plots for the charge redistributions suggest that the charge transfer between some parts of the intermediate regions between the germanene/silicene and the MoS_2 layers is obvious, suggesting much more than just the van der Waals interactions between the stacking sheets in the superlattices.

Methods

The present calculations are based on the density functional theory (DFT) and the projector-augmented wave (PAW) representations [27] as implemented in the Vienna *Ab Initio* Simulation Package (VASP) [28,29]. The exchange-correlation interaction is treated with the generalized gradient approximation (GGA) which is parameterized by Perdew-Burke-Ernzerhof formula (PBE) [30]. The standard DFT, where local or semilocal functionals lack the necessary ingredients to describe the nonlocal effects, has shown to dramatically underestimate the band gaps of various systems. In order to have a better description of the band gap, corrections should be added to the current DFT approximations [31,32]. On the other hand, as is well known, the popular density functionals are unable to describe correctly the vdW interactions resulting from dynamical correlations between fluctuating charge distributions [33]. Thus, to improve the description of the van der Waals interactions which might play an important role in the present layered superlattices, we included the vdW correction to the GGA calculations by using the PBE-D2 method [34]. The wave functions are expanded in plane waves up to a kinetic energy cutoff of 420 eV. Brillouin zone integrations are approximated by using the special ***k***-point sampling of Monkhorst-Pack scheme [35] with a Γ-centered $5 \times 5 \times 3$ grid. The cell parameters and the atomic coordinates of the superlattice models are fully relaxed until the force on each atom is less than 0.01 eV/Å.

Results and discussions

For the free-standing low-buckled germanene and silicene, the calculated lattice constants are 4.013 and 3.847 Å, respectively, which agree well with the reported values of 4.061 and 3.867 Å for germanene and silicene, respectively [36]. Our optimized lattice constant for a MoS_2 monolayer is 3.188 Å, which is the same as the previous calculated values by PBE calculations [37]. Although the lattice constants of germanene/silicene and MoS_2 monolayer are quite different, all of them do share the same primitive cell of hexagonal structure. For establishing the calculation models for Ger/MoS_2 and Sil/MoS_2 superlattices and to minimize the lattice mismatch between the stacking sheets, we have employed supercells consisting of 4×4 unit cells of germanene (and silicene) and 5×5 unit cells of MoS_2 monolayer in the *x*-*y* plane. Thus, we have $4a$(gemanene) = 16.052 Å, $4a$(silicene) = 15.388 Å, and $5a$(MoS_2 monolayer) = 15.940 Å, which lead to a lattice mismatch of around 0.70% between the germanene and MoS_2 layers and 3.46% between the silicene and MoS_2 layers. Compared with the hybrid systems investigated previously [38-42], the present lattice mismatch values are very small. In the calculations, first, the lattice constant of germanene/silicene ($4a_{ger/sil}$)

was set to match to that $(5a_{MoS_2})$ of the MoS_2 monolayer in the supercell. The supercells are then fully relaxed for both the lattice constants and the atomic geometry. The mismatch will finally disappear, leading to the commensurate systems. The superlattices we introduced in this work, by hybridizing germanene or silicene with MoS_2 monolayer, are shown in Figure 1. The supercells consist of alternate stacking of one germanene or silicene sheet and one MoS_2 monolayer, with 32 Ge or Si atoms, 25 Mo, and 50 S atoms per supercell. For a single Ge or Si atom adsorbed on a MoS_2 monolayer, there are three possible adsorption sites, i.e., the top site directly above a Mo atom, the top site directly above a S atom, and the hollow site above the center of a Mo-S hexagon. For the Ger/MoS_2 and Sil/MoS_2 superlattices, we consider two possible representative arrangements of germanene/silicene on the MoS_2 monolayer: (i) one Ge or Si atom in the supercell (4×4 unit cell) was set to sit directly on top of one Mo/S atom (the positions of all the other Ge or Si atoms will then be determined). In this way, there will be one Ge or Si atom in the supercell sitting on top of a S/Mo atom, too; see Figure 1c. (ii) One Ge or Si atom in the supercell was set to sit on the hollow site above the center of a hexagon of MoS_2, as shown in Figure 1d. From the present calculations, it is found that the binding energy differences between the above models of superlattices are very small (about 1 to 2 meV), which indicates that the energy of superlattice is not sensitive to the stacking of the atomic layers. Thus, in this paper, we show only the results of the configuration with one Ge or Si atom on top of the Mo or S atom. In all the stacking types, the 2D characteristics of the superlattice structures are kept, e.g., hexagonal atomic networks are seen in both Figure 1c,d which shows the fully optimized geometric structures of the supercells. Actually, the changes of the superlattice structures are quite small by atomic relaxations. The calculated lattice constants of Ger/MoS_2 and Sil/MoS_2 superlattices are 15.976 and 15.736 Å, respectively. In the Ger/MoS_2 superlattice, the germanene layers are compressed by 0.47% (from 4.013 to 3.994 Å) as compared to the corresponding isolated germanene, while the MoS_2 layers are expanded by 0.22% (from 3.188 to 3.195 Å) as compared to the free-standing MoS_2 monolayer. On the other hand, in the case of Sil/MoS_2 superlattice, the silicene layers in the superlattice are expanded by 2.26% (from 3.847 to 3.934 Å), while the MoS_2 layers in the supercell are reduced by 1.29% (from 3.188 to 3.147 Å) (see Table 1).

The averaged Mo-S bond lengths of the superlattices are calculated to be all around 2.400 Å (see Table 1). The averaged Ge-Ge/Si-Si bond lengths ($d_{Ge\text{-}Ge}/d_{Si\text{-}Si}$) in the relaxed superlattices are all around 2.400/2.300 Å, which are close to those in the free-standing germanene/silicene sheets (2.422/2.270 Å). Although the atomic bond lengths in the stacking planes are almost the same for Ger/MoS_2 and Sil/MoS_2 superlattices, the interlayer distances (d) exhibit relatively larger deviations (but still close to each other; see Table 1). A shorter interlayer distance d is found in the Ger/MoS_2 system, indicating that the Ge-MoS_2 interaction is stronger than the Si-MoS_2 interaction in the Sil/MoS_2 system. The Ge-S and Si-S atomic distances in the Ger/MoS_2 and Sil/MoS_2 superlattices are

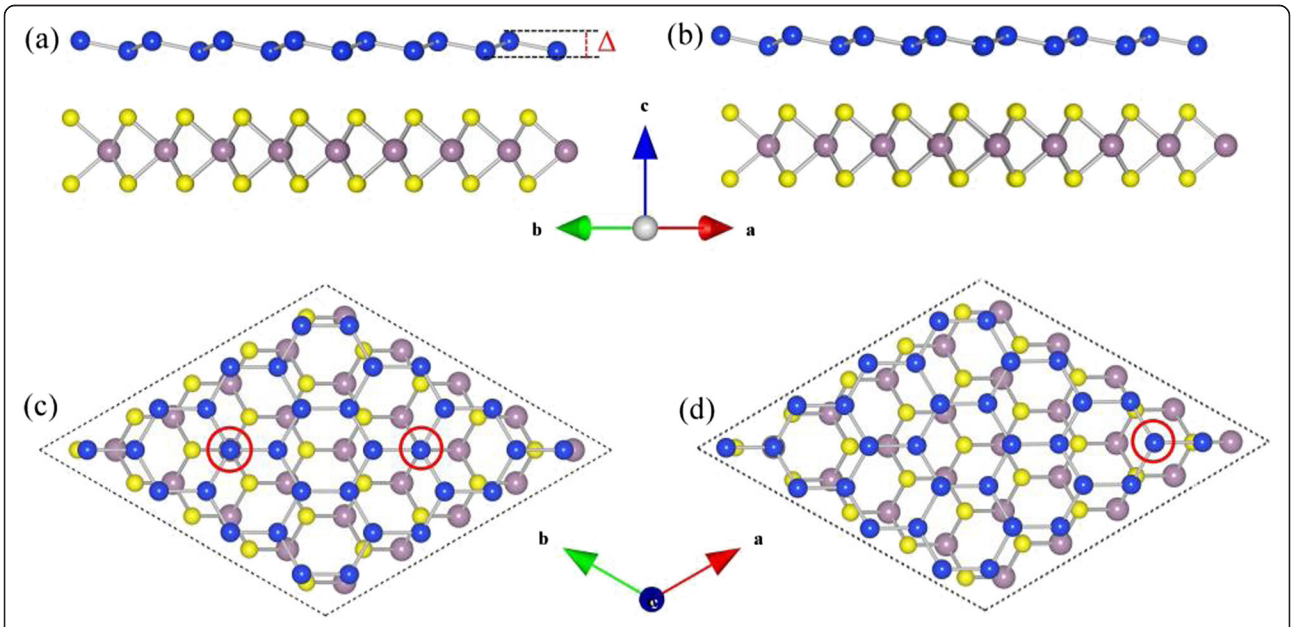

Figure 1 Side and top views of the two arrangements of germanene/silicene on MoS_2. (a, c) Top site configuration; **(b, d)** hollow site configuration. Ge/Si, Mo, and S atoms are represented by blue, purple, and yellow balls, respectively. The unit cells are shown by dashed lines.

Table 1 Binding energies, geometries, supercell lattice constants, averaged bond lengths, sheet thicknesses, and buckling of superlattices

System	E_b (per Ge/Si) (eV)	E_b (per MoS_2) (eV)	$a = b$ (Å)	c (Å)	$d_{Mo\text{-}S}$ (Å)	$d_{Ge\text{-}Ge}/d_{Si\text{-}Si}$ (Å)	$h_{S\text{-}S}$ (Å)	Δ_{Ge} (Å)	Δ_{Si} (Å)
Ger/MoS_2	0.277	0.354	15.976	9.778	2.410 to 2.430	2.420 to 2.440	3.129	0.782	
Sil/MoS_2	0.195	0.250	15.736	9.926	2.400 to 2.410	2.320 to 2.330	3.176		0.496
Germanene			16.052			2.422		0.706	
Silicene			15.388			2.270			0.468
MoS_2 monolayer			15.940		2.413		3.118		

Theoretical geometries of the isolated germanene, silicene, and MoS_2 monolayer are also listed. E_b, binding energies (per Ge/Si atom and per MoS_2); a, b, and c, supercell lattice constants; $d_{Mo\text{-}S}$, $d_{Ge\text{-}Ge}$, and $d_{Si\text{-}Si}$, averaged Mo-S and Ge-Ge/Si-Si bond lengths; $h_{S\text{-}S}$, sheet thicknesses of MoS_2; Δ_{Ge} and Δ_{Si}, amplitude of buckling of the germanene and silicene in the superlattices.

2.934 and 3.176 Å, respectively, where both values are shorter than 3.360 Å in the graphene/MoS_2 superlattice [6]. Such decreases of interlayer distances indicate the enhancement of interlayer interactions in the Ger/MoS_2 and Sil/MoS_2 superlattices as compared to the graphene/MoS_2 one. This can also explain why the amplitude of buckling (Δ) in the germanene/silicene layers of the superlattices become larger as compared to the free-standing germanene/silicene, i.e., Δ going from 0.706 to 0.782 Å in the germanene layers and from 0.468 to 0.496 Å in the silicene layers. The Ge-S and Si-S atomic distances in the Ger/MoS_2 and Sil/MoS_2 superlattices (2.934 and 3.176 Å) are much larger than 2.240 and 2.130 Å, the sum of the covalent atomic radius of Ge-S and Si-S atoms (the covalent radius is 1.220/1.110 Å for germanium/silicon and 1.020 Å for sulfur), which suggests that the interlayer bonding in the superlattices is not a covalent one.

To discuss the relative stabilities of the superlattices, the binding energy between the stacking sheets in the superlattice is defined as $E_b = -\left[E_{\text{supercell}} - (E_{MoS_2} + E_{Ger/Sil})\right]/N$, where $E_{\text{supercell}}$ is the total energy of the supercell, and E_{MoS_2} and $E_{Ger/Sil}$ are the total energies of a free-standing MoS_2 monolayer and an isolated germanene/silicene sheet, respectively. When $N = N(\text{Ge/Si}) = 32$, the number of Ge/Si atoms in the supercell, E_b is then the interlayer binding energy per Ge/Si atom. When $N = N(MoS_2) = 25$, the number of sulfur atoms in the supercell, then, E_b is the interlayer binding energy per MoS_2. The interlayer binding energies per Ge/Si atom and those per MoS_2 are presented in Table 1. E_{MoS_2} is calculated by using a 5×5 unit cell of the MoS_2 monolayer, and $E_{Ger/Sil}$ is calculated by using a 4×4 unit cell of the germanene/silicene. The binding energies between the stacking layers of the superlattices, calculated by the PBE-D2 method, are both relatively small, i.e., 0.277 eV/Ge and 0.195 eV/Si for the Ger/MoS_2 and Sil/MoS_2 superlattices, respectively (see Table 1). The small interlayer binding energies suggest weak interactions between the germanene/silicene and the MoS_2 layers. The binding energy also suggests that the interlayer interaction in Ger/MoS_2 superlattice is slightly stronger than that in the Sil/MoS_2 one. The interlayer binding energies are 0.354 eV/MoS_2 and 0.250 eV/MoS_2 for the Ger/MoS_2 and Sil/MoS_2 superlattices, respectively, both are larger than 0.158 eV/MoS_2 in the graphene/MoS_2 superlattice [6]. This is an indication that the mixed sp^2-sp^3 hybridization in the buckled germanene and silicene leads to stronger bindings of germanene/silicene with their neighboring MoS_2 atomic layers, when compared with the pure planar sp^2 bonding in the graphene/MoS_2 superlattice. In addition, the interlayer bindings become stronger and stronger in the superlattices of graphene/MoS_2 to silicene/MoS_2 and then to germanene/MoS_2 monolayer.

Figure 2 shows the band structures of various 2D materials, e.g., the bands of flat germanene/silicene compared with low-buckled germanene/silicene. The band structure of flat silicene is similar to that of low-buckled one. In both kinds of silicene, the systems are semimetal with linear bands around the Dirac point at the K point of the Brillouin zone. On the other hand, the band structure of flat germanene is quite different from that of low-buckled one. The flat germanene is metallic, and the Dirac point does not sit at the Fermi level (but above the E_F). The band structure of low-buckled germanene, however, is similar to that of the low-buckled silicene. To help understand the electronic band structures of the superlattices and the contribution of each atomic layer to the band structures, we present in Figure 3 the band structures of Ger/MoS_2 and Sil/MoS_2 superlattices, together with those of the independent low-buckled germanene/silicene and MoS_2 monolayer sheets. The band structures of free-standing buckled germanene/silicene and MoS_2 sheets (Figure 3a,b,c) are calculated by using 4×4 and 5×5 supercells, respectively, in order to compare with the band structures of the superlattices directly. The band structures of the Ger/MoS_2 and Sil/MoS_2 superlattices are presented in Figure 3d,e, where the contributions of the germanene/silicene and MoS_2 monolayers to the band structures of the superlattices are shown with blue and green dots (where the size of

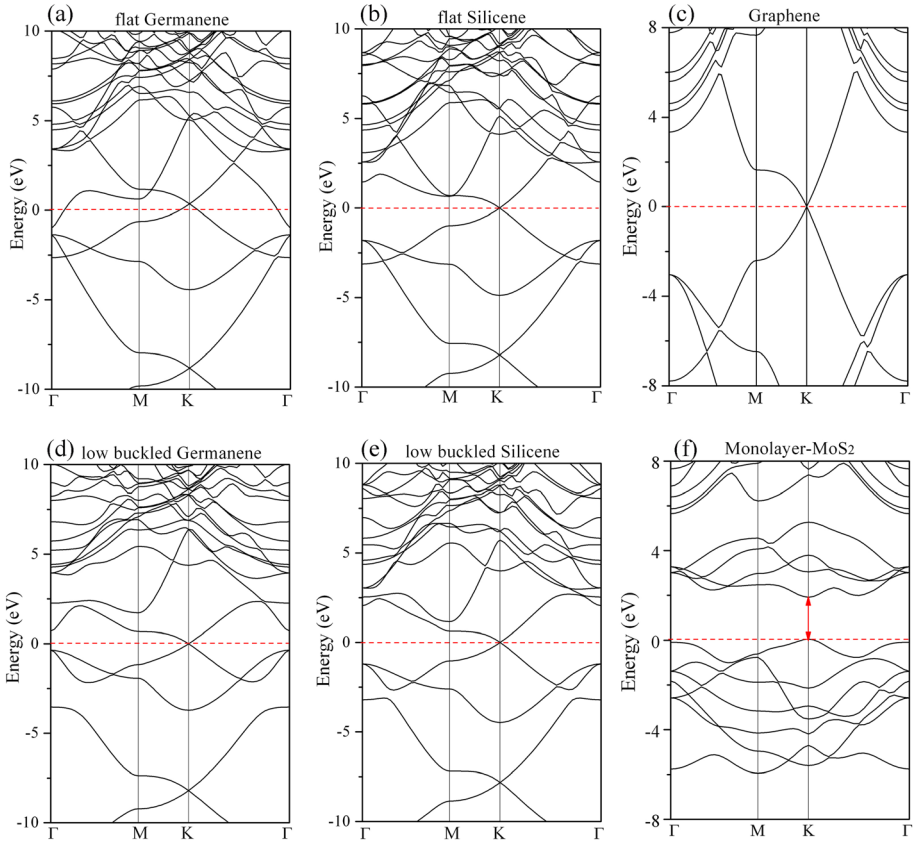

Figure 2 Band structures of various 2D materials. (a) Flat germanene, **(b)** flat silicene, **(c)** graphene, **(d)** low-buckled germanene, **(e)** low-buckled silicene, and **(f)** MoS_2 monolayer.

dots are proportional to the contributions), respectively. In general, the outlines of the band structures of the two superlattices seem to be similar to the 'rigid sum' of the bands of each constituent (i.e., the bands of independent germanene/silicene and MoS_2 sheets), indicating that the couplings between the stacking sheets are relatively weak. However, new important characters in the band structures of the superlattices appear. Both the Ger/MoS_2 and Sil/MoS_2 superlattice systems manifest metallic properties, since there are several bands crossing the Fermi level. In fact, in the superlattice systems, the Dirac points of the free-standing germanene/silicene (at the *K* point) move upward slightly above the Fermi level; at the same time, the Dirac points at the *H* point (*H* is above *K* in the *z*-direction in the BZ) move downward slightly below the Fermi level. Such shifts of Dirac points lead to partially occupied bands in the superlattices, also implying charge transfer around *K* point to the *H* point in the BZ. The bands crossing the Fermi level are contributed mainly by the germanene/silicene layers rather than the MoS_2 sheets in both the Ger/MoS_2 and Sil/MoS_2 superlattices, except that small contributions from MoS_2 sheet are visible around the *H* point. Contributions from the MoS_2 layers to the electronic states around the Fermi level are more significantly visible in the system of Ger/MoS_2 than in the Sil/MoS_2 system. The feature of energy bands suggests that the electronic conduction of the superlattices exists mainly in the *x*-*y* plane and is almost contributed by the germanene/silicene sheets rather than the MoS_2 sheets, namely, the superlattices are compounds made with alternate stacking of conductive germanene/silicene layers and nearly insulating MoS_2 sheets. This is different from the graphene/MoS_2 superlattice, in which both graphene and MoS_2 layers can be conductive, resulting from the charge transfer between the graphene and MoS_2 sheets [6]. Moreover, according to the detailed band structures inserted in the vicinity of Figure 3d,e, we found that small band gaps opened up at the *K* point of the BZ (the Dirac point of the germanene/silicene), which is now above the Fermi level. The gaps that opened for the Ger/MoS_2 and Sil/MoS_2 superlattices are 24 and 7 meV, respectively (the sizes of the gaps could be well underestimated). Since the electronic states around *K* point are almost fully contributed from the germanene/silicene layers, the gaps that opened for the superlattices are due to the interactions between the germanene/silicene layers only. In other words, the formation of the small-

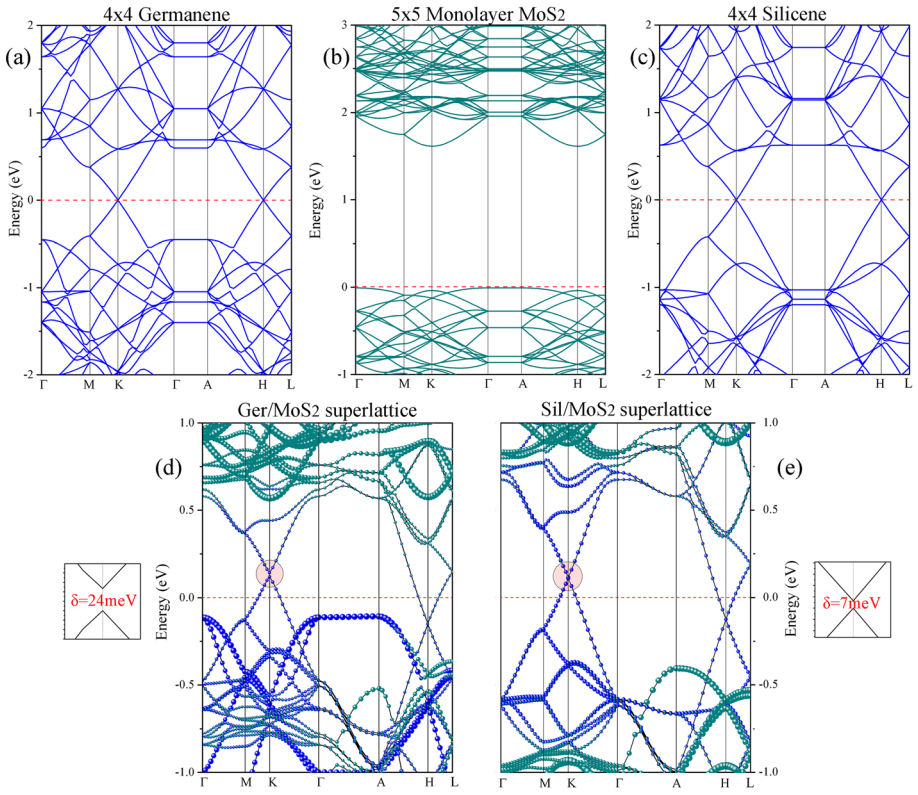

Figure 3 Band structures of free-standing. (a) Germanene calculated with a 4 × 4 supercell, **(b)** MoS_2 monolayer calculated with a 5 × 5 supercell, and **(c)** silicene calculated with a 4 × 4 supercell. **(d, e)** The band structures of Ger/MoS_2 and Sil/MoS_2 superlattices, respectively. The contributions from the germanene/silicene and MoS_2 layers to the band structures of the superlattices are shown with blue and green dots, respectively. The detailed band structures in the vicinity of the opened band gap are inserted. Red dashed lines represent the Fermi level.

sized band gaps at the *K* point is due to the symmetry breaking within the germanene/silicene layers caused by the introduction of the MoS_2 sheets in the formation of superlattices [43-46].

To further explore the bonding nature and the charge transfer in the Ger/MoS_2 and Sil/MoS_2 superlattices, the contour plots of the charge density differences ($\Delta\rho_1$) on the planes passing through germanene, silicene, and sulfur layers (in the *x-y* plane) are shown in Figure 4a,b,c,d. The deformation charge density $\Delta\rho_1$ is defined as $\Delta\rho_1\left(\vec{r}\right) = \rho\left(\vec{r}\right) - \sum_{\mu}\rho_{\mathrm{atom}}\left(\vec{r} - \vec{R}_{\mu}\right)$, where $\rho\left(\vec{r}\right)$ represents the total charge density of the superlattice and $\sum_{\mu}\rho_{\mathrm{atom}}\left(\vec{r} - \vec{R}_{\mu}\right)$ is the superposition of atomic charge densities. The deformation charge density shown in Figure 4a,b,c,d exhibited that the formation of the Ger/MoS_2 and Sil/MoS_2 superlattices did not distort significantly the charge densities of germanene, silicene, or sulfur layers, when compared with the deformation charge density in the free-standing germanene, silicene layers, or sulfur layers in the MoS_2 sheets (not shown).

Figure 4e,f shows the contour plots of $\Delta\rho_1$ on the planes perpendicular to the atomic layers and passing through Mo-S, Ge-Ge, or Si-Si bonds in the Ger/MoS_2 and Sil/MoS_2 superlattices. As in the case of isolated germanene/silicene or MoS_2 monolayer (not presented), the atomic bonding within each atomic layer in both the superlattices are mainly covalent bonds. Moreover, shown in Figure 4g,h, we also present the charge density differences ($\Delta\rho_2$) of the same planes as in Figure 4e,f. The $\Delta\rho_2$ is defined as $\Delta\rho_2\left(\vec{r}\right) = \rho\left(\vec{r}\right) - \rho_{\mathrm{slab}}(\mathrm{Ger/Sil}) - \rho_{\mathrm{slab}}(\mathrm{MoS_2})$, where $\rho\left(\vec{r}\right)$, ρ_{slab}(Ger/Sil), and $\rho_{\mathrm{slab}}(\mathrm{MoS_2})$ are the charge densities of the superlattice, the germanene/silicene, and the MoS_2 slabs, respectively. In the calculation of ρ_{slab}(Ger/Sil) and ρ_{slab}(MoS_2), we employ the same supercell that is used for the superlattice. For calculating the ρ_{slab}(Ger/Sil), the MoS_2 slabs in the superlattice are removed and the charge densities of the germanene/silicene slabs are then calculated including a structure relaxation. For calculating $\rho_{\mathrm{slab}}(\mathrm{MoS_2})$, the germanene/silicene layers are then removed. Such a $\Delta\rho_2$ can clearly demonstrate

the charge transfer between the stacking layers in the superlattices. Figure 4g,h indicates that the charge transfer happened mainly within the germanene/silicene and the MoS_2 layers (intra-layer transfer), as well as in some parts of the intermediate regions between the germanene/silicene and MoS_2 layers (inter-layer transfer). This is somewhat different from the graphene/MoS_2 superlattice, where the charge transfer from the graphene sheet to the intermediate region between the graphene and MoS_2 layers is much more significantly visible [6]. Such charge redistributions in the Ger/MoS_2 and Sil/MoS_2 systems, shown in Figure 4, indicate that the interactions between some parts of the stacking atomic layers are relatively strong, suggesting much more than just the van der Waals interactions between the stacking sheets.

Conclusions

In summary, the first principles calculations based on density functional theory including van der Waals corrections have been carried out to study the structural and electronic properties of superlattices composed of germanene/silicene and MoS_2 monolayer. Due to the relatively weak interactions between the stacking layers, the distortions of the geometry of germanene, silicene and MoS_2 layers in the superlattices are all relatively small. Unlike the free-standing germanene or silicene which is a semimetal and the MoS_2 monolayer which is a semiconductor, both the Ger/MoS_2 and Sil/MoS_2 superlattices exhibit metallic electronic properties. Due to symmetry breaking, small band gaps are opened up at the K point of the BZ for both the superlattices. Charge transfer happened mainly within the

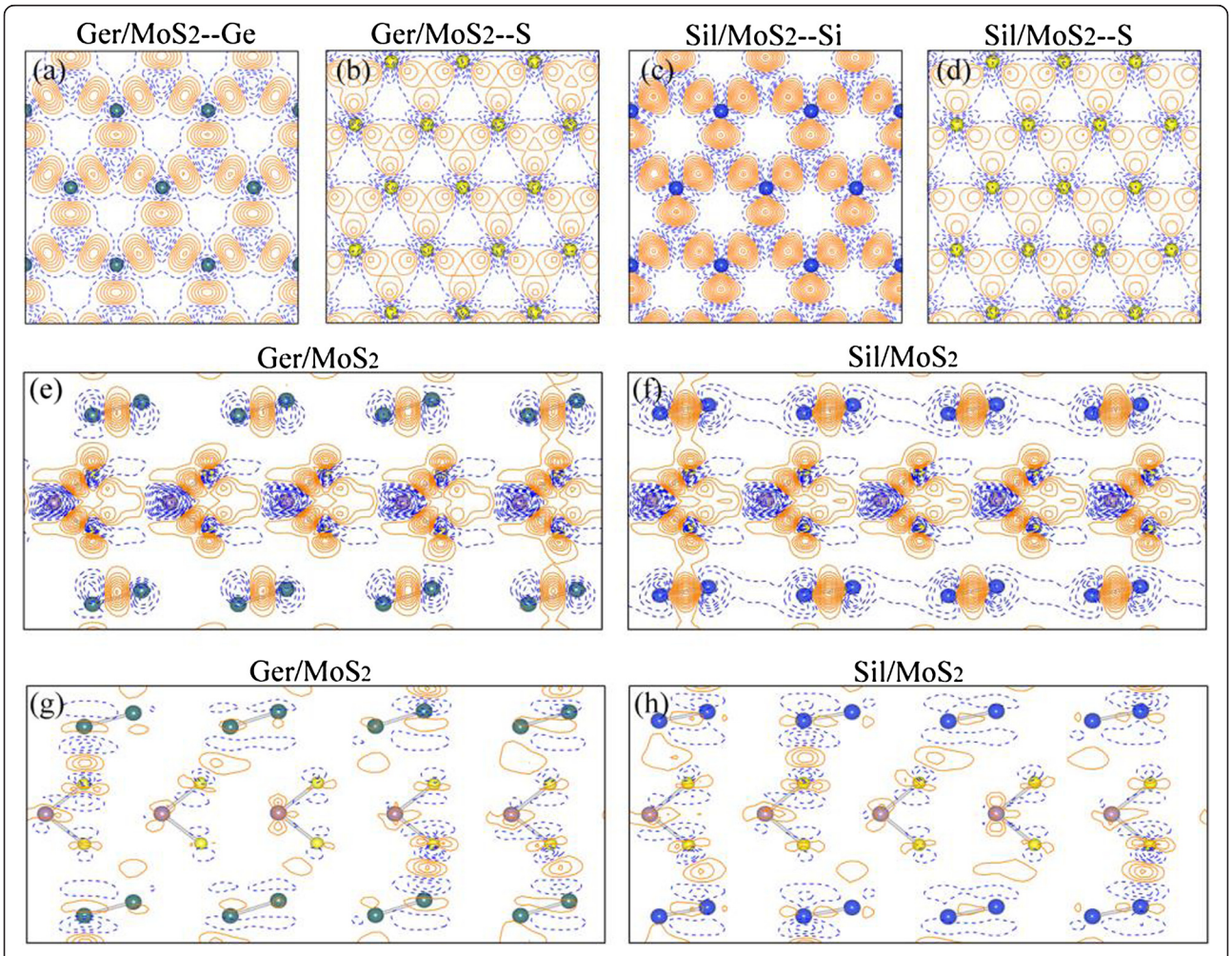

Figure 4 Contour plots of the deformation charge density ($\Delta\rho_1$ and $\Delta\rho_2$). (a, b) $\Delta\rho_1$ on the planes passing through germanene and sulfur layers in the Ger/MoS_2 superlattice. **(c, d)** $\Delta\rho_1$ on the planes passing through silicene and sulfur layers in the Sil/MoS_2 system. **(e, f)** $\Delta\rho_1$ on the planes perpendicular to the atomic layers and passing through Mo-S, Ge-Ge, or Si-Si bonds in the superlattices. **(g, h)** Charge density differences ($\Delta\rho_2$) of the same planes as those in **(e)** and **(f)**. The green/blue, purple, and yellow balls represent Ge/Si, Mo, and S atoms, respectively. Orange and blue lines correspond to $\Delta\rho > 0$ and $\Delta\rho < 0$, respectively.

germanene/silicene and the MoS_2 layers (intra-layer charge transfer), as well as in some parts of the intermediate regions between the germanene/silicene and MoS_2 layers (inter-layer charge transfer). Such charge redistributions indicate that the interactions between some parts of the stacking layers are relatively strong, suggesting more than just the van der Waals interactions between the stacking sheets.

Competing interests
The authors declare that they have no competing interests.

Authors' contributions
XL carried out the density functional theory simulation, performed the data analysis, and drafted the manuscript. SW and SZ helped discuss the data analysis of the superlattice. ZZ organized the final manuscript. All authors read and approved the final manuscript.

Acknowledgements
This work is supported by the National 973 Program of China (Grant No. 2011CB935903) and the National Natural Science Foundation of China under Grant No. 11104229, 21233004.

Author details
[1]Department of Physics, Xiamen University, Xiamen 361005, China. [2]Institute of Theoretical Physics and Astrophysics, Xiamen University, Xiamen 361005, China. [3]State Key Laboratory of Theoretical Physics, Institute of Theoretical Physics, Chinese Academy of Sciences, Beijing 100864, China.

Received: 26 January 2014 Accepted: 27 February 2014
Published: 8 March 2014

References
1. Xu Y, Liu Y, Chen H, Lin X, Lin S, Yu B, Luo J: **Ab initio study of energy-band modulation in graphene-based two-dimensional layered superlattices.** *J Mater Chem* 2012, **22:**23821–23829.
2. Chang K, Chen WX: **L-cysteine-assisted synthesis of layered MoS_2/graphene composites with excellent electrochemical performances for lithium ion batteries.** *ACS Nano* 2011, **5:**4720–4728.
3. Chang K, Chen WX, Ma L, Li H, Huang FH, Xu ZD, Zhang QB, Lee JY: **Graphene-like MoS_2/amorphous carbon composites with high capacity and excellent stability as anode materials for lithium ion batteries.** *J Mater Chem* 2011, **21:**6251–6257.
4. Chang K, Chen WX: **In situ synthesis of MoS_2/graphene nanosheet composites with extraordinarily high electrochemical performance for lithium ion batteries.** *Chem Commun* 2011, **47:**4252–4254.
5. Chang K, Chen WX: **Single-layer MoS_2/graphene dispersed in amorphous carbon: towards high electrochemical performances in rechargeable lithium ion batteries.** *J Mater Chem* 2011, **21:**17175–17184.
6. Li XD, Yu S, Wu SQ, Wen YH, Zhou S, Zhu ZZ: **Structural and electronic properties of superlattice composed of graphene and monolayer MoS_2.** *J Phys Chem C* 2013, **117:**15347–15353.
7. Akiyama M, Kawarada Y, Kaminishi K: **Growth of GaAs on Si by MOVCD.** *J Cryst Growth* 1984, **68:**21–26.
8. Novoselov KS, Geim AK, Morozov SV, Jiang D, Zhang Y, Dubonos SV, Grigorieva IV, Firsov AA: **Electric field effect in atomically thin carbon films.** *Science* 2004, **306:**666–669.
9. Novoselov KS, Jiang D, Schedin F, Booth TJ, Khotkevich VV, Morozov SV, Geim AK: **Two-dimensional atomic crystals.** *Proc Natl Acad Sci U S A* 2005, **102:**10451–10453.
10. Dean CR, Young AF, Meric I, Lee C, Wang L, Sorgenfrei S, Watanabe K, Taniguchi T, Kim P, Shepard KL, Hone J: **Boron nitride substrates for high-quality graphene electronics.** *Nat Nanotechnol* 2010, **5:**722–726.
11. Radisavljevic B, Radenovic A, Brivio J, Giacometti V, Kis A: **Single-layer MoS_2 transistors.** *Nat Nanotechnol* 2011, **6:**147–150.
12. Britnell L, Gorbachev RV, Jalil R, Belle BD, Schedin F, Mishchenko A, Georgiou T, Katsnelson MI, Eaves L, Morozov SV, Peres NMR, Leist J, Geim AK, Novoselov KS, Ponomarenko LA: **Field-effect tunneling transistor based on vertical graphene heterostructures.** *Science* 2012, **335:**947–950.
13. Britnell L, Gorbachev RV, Jalil R, Belle BD, Schedin F, Katsnelson MI, Eaves L, Morozov SV, Mayorov AS, Peres NMR, Neto AHC, Leist J, Geim AK, Ponomarenko LA, Novoselov KS: **Electron tunneling through ultrathin boron nitride crystalline barriers.** *Nano Lett* 2012, **12:**1707–1710.
14. Kahng K, Sze SM: **A floating gate and its application to memory devices.** *IEEE Trans Electron Devices* 1967, **14:**629–629.
15. Ataca C, Ciraci S: **Functionalization of single-layer MoS_2 honeycomb structures.** *J Phys Chem C* 2011, **115:**13303–13311.
16. Bertolazzi S, Krasnozhon D, Kis A: **Nonvolatile memory cells based on MoS_2/graphene heterostructures.** *ACS Nano* 2013, **7:**3246–3252.
17. Cahill DG, Ford WK, Goodson KE, Mahan GD, Majumdar A, Maris HJ, Merlin R, Phillpot SR: **Nanoscale thermal transport.** *J Appl Phys* 2003, **93:**793–818.
18. Wu BJ, Kuo LH, Depuydt JM, Haugen GM, Haase MA, Salamancariba L: **Growth and characterization of II–VI blue light-emitting diodes using short period superlattices.** *Appl Phys Lett* 1996, **68:**379–381.
19. Rees P, Helfernan JF, Logue FP, Donegan JF, Jordan C, Hegarty J, Hiei F, Ishibashi A: **High temperature gain measurements in optically pumped ZnCdSe-ZnSe quantum wells.** *IEE Proc Optoelectron* 1996, **143:**110–112.
20. Cahangirov S, Topsakal M, Akturk E, Sahin H, Ciraci S: **Two- and one-dimensional honeycomb structures of silicon and germanium.** *Phys Rev Lett* 2009, **102:**236804. 4.
21. Sahin H, Cahangirov S, Topsakal M, Bekaroglu E, Akturk E, Senger RT, Ciraci S: **Monolayer honeycomb structures of group-IV elements and III-V binary compounds: first-principles calculations.** *Phys Rev B* 2009, **80:**155453.
22. Liu CC, Feng W, Yao Y: **Quantum spin Hall effect in silicene and two-dimensional germanium.** *Phys Rev Lett* 2011, **107:**076802–076804.
23. Yang B, Liu JL, Wang KL, Chen G: **Simultaneous measurements of Seebeck coefficient and thermal conductivity across superlattice.** *Appl Phys Lett* 2002, **80:**1758–1760.
24. Liu CK, Yu CK, Chien HC, Kuo SL, Hsu CY, Dai MJ, Luo GL, Huang SC, Huang MJ: **Thermal conductivity of Si/SiGe superlattice films.** *J Appl Phys* 2008, **104:**114301–114308.
25. Huxtable ST, Abramson AR, Tien CL, Majumdar A, LaBounty C, Fan X, Zeng G, Bowers JE, Shakouri A, Croke ET: **Thermal conductivity of Si/SiGe and SiGe/SiGe superlattices.** *Appl Phys Lett* 2002, **80:**1737–1739.
26. Laref A, Belgoumene B, Aourag H, Maachou M, Tadjer A: **Electronic structure and interfacial properties of ZnSe/Si, ZnSe/Ge, and ZnSe/SiGe superlattices.** *Superlattice Microst* 2005, **37:**127–137.
27. Kresse G, Joubert D: **From ultrasoft pseudopotentials to the projector augmented-wave method.** *Phys Rev B* 1999, **59:**1758–1775.
28. Kresse G, Furthmüller J: **Efficiency of ab-initio total energy calculations for metals and semiconductors using a plane-wave basis set.** *Comput Mater Sci* 1996, **6:**15–50.
29. Kresse G, Furthmüller J: **Efficient iterative schemes for ab initio total-energy calculations using a plane-wave basis set.** *Phys Rev B* 1996, **54:**11169–11186.
30. Perdew JP, Burke K, Ernzerhof M: **Generalized gradient approximation made simple.** *Phys Rev Lett* 1996, **77:**3865–3868.
31. Perdew JP, Levy M: **Physical content of the exact Kohn-Sham orbital energies: band gaps and derivative discontinuities.** *Phys Rev Lett* 1983, **51:**1884–1887.
32. Sham LJ, Schluter M: **Density-functional theory of the energy Gap.** *Phys Rev Lett* 1983, **51:**1888–1891.
33. Ivanovskaya VV, Heine T, Gemming S, Seifert G: **Structure, stability and electronic properties of composite $Mo_{1-x}Nb_xS_2$ nanotubes.** *Phys Status Solidi B* 2006, **243:**1757–1764.
34. Grimme S: **Semiempirical GGA-type density functional constructed with a long-range dispersion correction.** *J Comput Chem* 2006, **27:**1787–1799.
35. Monkhorst HJ, Pack J: **Special points for Brillouin-zone integrations.** *Phys Rev B* 1976, **13:**5188–5192.
36. Garcia JC, de Lima DB, Assali LVC, Justo JF: **Group IV graphene- and graphane-like nanosheets.** *J Phys Chem C* 2011, **115:**13242–13246.
37. Ding Y, Wang Y, Ni J, Shi L, Shi S, Tang W: **First principles study of structural, vibrational and electronic properties of graphene-like MX_2 (M = Mo, Nb, W, Ta; X = S, Se, Te) monolayers.** *Physica B* 2011, **406:**2254–2260.
38. Seifert G, Terrones H, Terrones M, Jungnickel G, Frauenheim T: **On the electronic structure of WS_2 nanotubes.** *Solid State Commun* 2000, **114:**245–248.
39. Li W, Chen J, He Q, Wang T: **Electronic and elastic properties of MoS_2.** *Physica B* 2010, **405:**2498–2502.

40. Lebégue S, Eriksson O: **Electronic structure of two-dimensional crystals from ab initio theory.** *Phys Rev B* 2009, **79:**115409. 4.
41. Li Y, Zhou Z, Zhang S, Chen Z: **MoS_2 nanoribbons: high stability and unusual electronic and magnetic properties.** *J Am Chem Soc* 2008, **130:**16739–16744.
42. Seifert G, Terrones H, Terrones M, Jungnickel G, Frauenheim T: **Structure and electronic properties of MoS_2 nanotubes.** *Phys Rev Lett* 2000, **85:**146–149.
43. O'Hare A, Kusmartsev FV, Kugel KI: **A stable "flat" form of two-dimensional crystals: could graphene, silicene, germanene be minigap semiconductors?** *Nano Lett* 2012, **12:**1045–1052.
44. Ni Z, Liu Q, Tang K, Zheng J, Zhou J, Qin R, Gao Z, Yu D, Lu J: **Tunable bandgap in silicene and germanene.** *Nano Lett* 2012, **12:**113–118.
45. Ye M, Quhe R, Zheng J, Ni Z, Wang Y, Yuan Y, Tse G, Shi J, Gao Z, Lu J: **Tunable band gap in germanene by surface adsorption.** *Phys E* 2014, **59:**60–65.
46. Quhe R, Fei R, Liu Q, Zheng J, Li H, Xu C, Ni Z, Wang Y, Yu D, Gao Z, Lu J: **Tunable and sizable band gap in silicene by surface adsorption.** *Sci Rep* 2012, **2:**853.

doi:10.1186/1556-276X-9-110
Cite this article as: Li *et al.*: Structural and electronic properties of germanene/MoS_2 monolayer and silicene/MoS_2 monolayer superlattices. *Nanoscale Research Letters* 2014 **9**:110.